



Project Avigator

NASA University Student Launch Initiative 2024 FRR Addendum

University of Florida

Swamp Launch Rocket Team
571 Gale Lemerand Dr, Gainesville, FL 32611
MAE-C Room 134
March 28th, 2024



Table of Contents

1. Summary of Report.....	3
1.1 Team Summary	3
1.1.1 Hours.....	3
1.2 Purpose of Flight.....	3
1.3 Flight Summary Information.....	3
1.4 Changes Made Since FRR	4
1.4.1 Changes in Vehicle Design.....	4
1.4.2 Changes in Payload Design	4
2. Payload Demonstration Flight Results.....	4
2.1 Summary.....	4
2.2 Designed Payload Mission Sequence.....	4
2.3 Designed Payload Retention System	5
2.4 Flight Data	8
2.4.1 Landed Configuration	8
2.4.2 Descent Values	13
2.5 Payload Functionality.....	13
2.5.1 Functional Systems	13
2.5.2 Off-Nominal Events	17
2.6 Payload Hardware Damage	17
2.6.1 Mechanical Hardware	17
2.6.2 Electrical Hardware	17
2.7 Lessons Learned.....	17



1. Summary of Report

1.1 Team Summary

Swamp Launch Rocket Team
MAE-C Room 134
571 Gale Lemerand Drive
Gainesville, FL 32611
Primary Contact: Stephanie Baldwin (baldwinstephanie@ufl.edu)

1.1.1 Hours

FRR Addendum Hours: 109

1.2 Purpose of Flight

One flight was conducted after the Flight Readiness Review deadline to fulfill the requirements for the Payload Demonstration Flight.

1.3 Flight Summary Information

Flight information for the Payload Demonstration Flight is tabulated (Table 1). Off-nominal events are detailed in 2.5.2 Off-Nominal Events.

Payload Demonstration Flight Overview	
Date of Flight	March 16 th , 2024
Flight Location	Palm Bay, FL (Tripoli Prefecture 73/NAR Section 342)
Motor Flown	AeroTech L1150
Ballast Flown	0 lbs
Final Payload Flown?	Yes
Air Brake System Status	N/A
Official Target Altitude	5000 ft
Predicted Altitude from Simulations	4625 ft
Measured Altitude	4671 ft

Table 1: Payload Demonstration Flight Summary

The launch day conditions were recorded and used in simulations to determine the predicted flight performance (Table 2).

Launch Conditions	
Wind Speed	5 mph
Launch Angle	5°
Launch Rod Length	144 in
Latitude	27.9°N
Longitude	80.7°W
Elevation	16.4 ft
Temperature	86°F
Pressure	1 atm

Table 2: Payload Demonstration Flight Launch Day Conditions



1.4 Changes Made Since FRR

1.4.1 Changes in Vehicle Design

No changes were made to the structural components of the launch vehicle after the Flight Readiness Review.

A small change was made to the recovery system design wherein small sections of foam tubing were wrapped around the shock cord where it meets the edge of the airframe. This change mitigates the possibility of airframe zippering and was approved by NASA.

1.4.2 Changes in Payload Design

While preparing the payload retention system, the forward sabot, which held the front side of the payload, was removed. This was necessary because it interfered with the propeller assembly and prevented the payload from fitting completely inside the payload bay.

The harness attaching the forward and aft sabots to the payload bay were changed from $\frac{1}{4}$ in Kevlar recovery harness to paracord. This was done to reduce the size and weight of the harness.

During the test flight, a functionally identical, older version of the cockpit was used for testing.

2. Payload Demonstration Flight Results

2.1 Summary

The individual parts of the payload functioned as intended. The payload and ground station were able to maintain radio contact, with the ground station receiving the live video feed and the payload responding to radio commands. The payload retention system servos retracted to let the door open at 400 ft, but the payload did not deploy itself from the payload bay, likely because it was wedged too tightly into the bay. Because the payload was unable to fully deploy, complete payload functionality was unable to be demonstrated.

2.2 Designed Payload Mission Sequence

Figure 1 shows the designed payload mission sequence. After the payload has been assembled in final configuration, it is to be loaded into the payload section of the launch vehicle. The launch vehicle, also in final configuration, is then set up on the launch pad and launch is initiated (Step 1). After launch, the flight controller subsystem is turned on by the microprocessor subsystem, as detailed in FRR (Step 2). If video overlaid with telemetry data is received at the ground station (Step 3), RSO permission is given, and the temperature is below 158 °F (Step 4), the payload is armed to be deployed at 400 ft (Step 5). After deployment the payload is piloted to the ground while meeting the kinetic energy requirements (NASA Requirement 3.3, Step 6). After the payload has landed and it is safe to recover (Step 7), the payload will be recovered. Following recovery, the data collected by the microprocessor subsystem will be retrieved and analyzed to determine if the mission was successful. If a force greater than 9 gs is detected for more than 5 seconds or if the kinetic energy requirements are violated, the mission will be considered a failure.

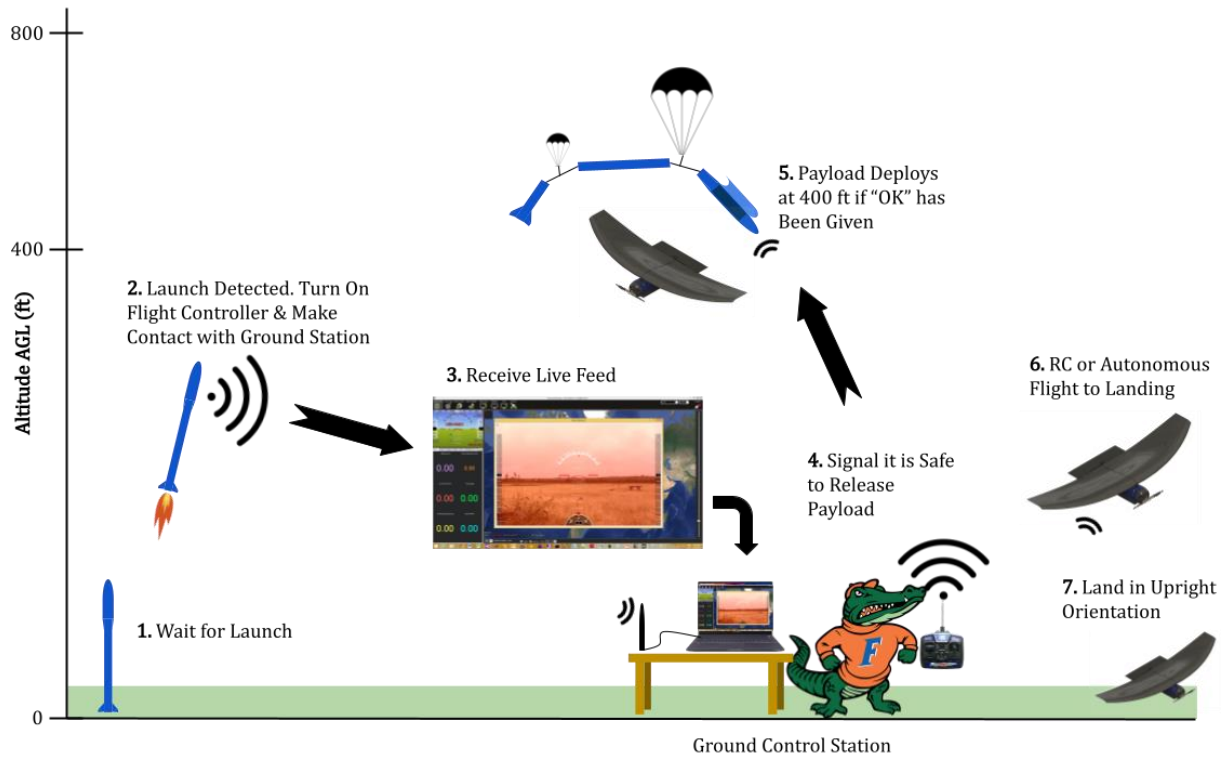


Figure 1: Payload Concept of Operations

2.3 Designed Payload Retention System

The payload retention system is housed within the bay of the payload airframe and consists of a payload door assembly that hinges open. This system is controlled by two rack and pinion mechanisms that extend and retract a beam that interferes with the payload door half bulkheads in the payload door assembly. Additionally, the payload is retained within the launch vehicle during flight with sabots that are attached to the launch vehicle.

The payload is held within the launch vehicle during flight with sabots, which were made from two-part expanding foam. The forward sabot has a rounded pocket that interfaces with the spherical cockpit and contains a cutout to provide clearance for the central prop attachment. The aft sabot features a wedge-shaped pocket that matches the surface of the aft of the payload and contains a slot for the rudder to slide into. These components were tethered to the inside of the vehicle with a short length of paracord, allowing the sabots to remain within the launch vehicle after deployment of the payload (Figure 2).

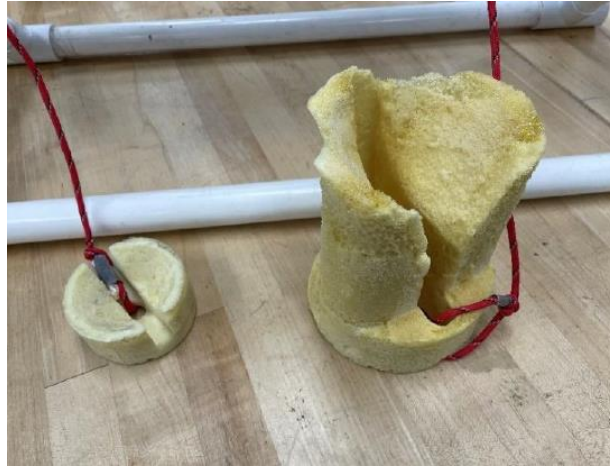


Figure 2: Payload Sabots

A set of two rack and pinion mechanisms were installed within the payload bay to control the ejection of the payload (Figure 3). The rack and pinion mechanism consists of a Miuzei 20kg servo motor attached to the servo mount. A pinion gear attached to the spline of the servo motor, which interfered with the teeth of the gear rack, allowing it to move linearly. A gear rack fastened to the flat beam, with its linear actuating movement being constrained within a servo mount.



Figure 3: Rack and Pinion Mechanism Assembled

The rack and pinion mechanisms used for the payload retention system were epoxied with JB Weld onto the payload forward and aft bulkheads (Figure 4). The battery powering these mechanisms was also epoxied onto the payload aft bulkhead. Once the battery was connected, the wires and recovery harness for the aft sabot passed through a hole on the payload aft bulkhead. This bulkhead was then fastened into the forwardmost centering ring of the transition assembly with two 1/4-20 head screws (Figure 5).

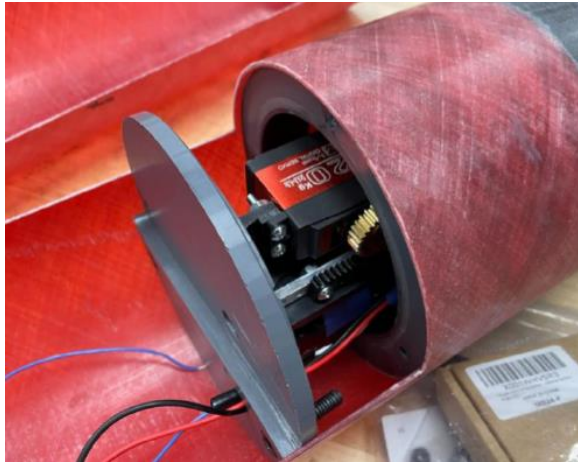


Figure 4: Aft Payload Bulkhead with Payload Retention System Electronics Mounted to the Aft End



Figure 5: Payload Aft Bulkhead Showing Wires, Attached Recovery Harness, and Beam from Rack and Pinion Mechanism

The payload door assembly was then fastened to the payload forward and aft bulkheads with shoulder screws. This point acts as the pivoting point of this assembly for the door to open and close (Figure 6).

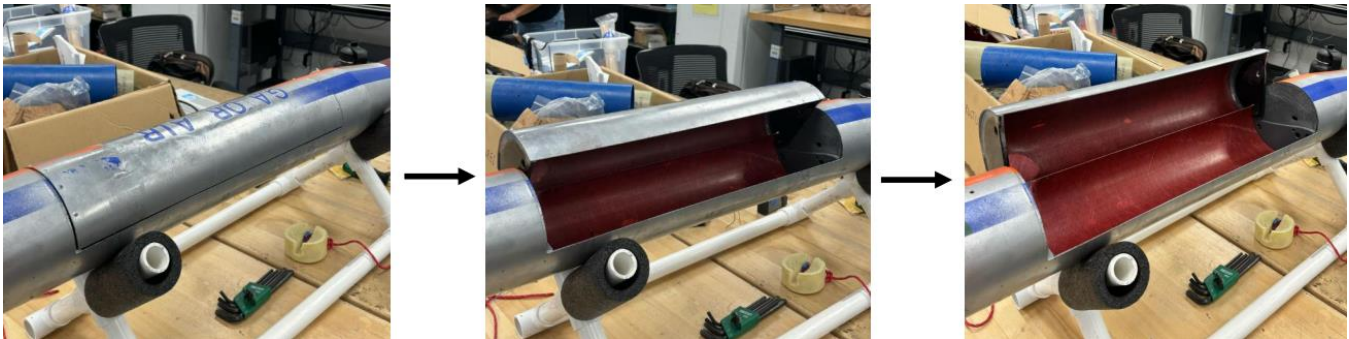


Figure 6: Payload Door Assembly Hinging Opened

Once the payload retention system was fully assembled, the payload was rolled and placed within the payload bay (Figure 7). However, while preparing the payload retention system during demonstration, the forward sabot, which held the front side of the payload, was removed. This was necessary because it interfered with the propeller assembly and prevented the payload from fitting completely inside the payload bay (Figure 8).



Figure 7: Sabots Attached to Launch Vehicle with Recovery Harnesses



Figure 8: Payload Rolled and Placed Inside Payload Bay

2.4 Flight Data

During flight, two altimeters were utilized. The main altimeter was the Stratologger CF, and the secondary altimeter was the MissileWorks RRC3. Due to an error in the secondary altimeter where the data written during flight failed to save, only data from the main altimeter was available for the Payload Demonstration Flight. Despite this failure to write data, both the backup ejection charges connected to the backup altimeter successfully detonated. The altitude and velocity profiles of the OpenRocket simulation and the Stratologger CF flight data are shown in Figure 9 and Figure 10. Some noise is present in the velocity flight data during the descent under drogue, and especially around the time of main parachute deployment, but this noise was deemed insignificant and was caused by the fast-sampling rate, which propagated small errors in the measured altitude to larger velocity deviations.

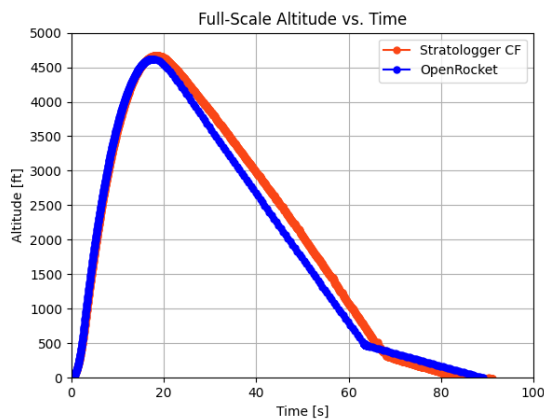


Figure 9: PDF Resulting Altitude vs. Time

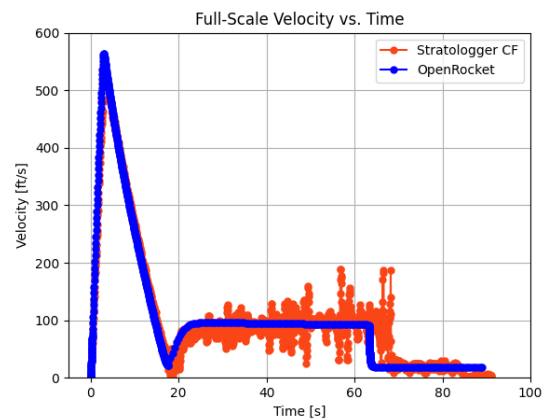


Figure 10: PDF Resulting Velocity vs. Time

2.4.1 Landed Configuration

2.4.1.1 Launch Vehicle

The launch vehicle was undamaged (Figure 11 - Figure 20).



Figure 11: Payload Section Viewed From Aft with Unlocked Door



Figure 12: Payload Section Viewed From Nosecone with Unlocked Door



Figure 13: Central Section



Figure 14: Main Parachute with Parachute Protector



Figure 15: Main Parachute



Figure 16: Drogue Parachute



Figure 17: Aft Section Viewed from Forward



Figure 18: Aft Section Viewed from Aft



Figure 19: Entire Landed Configuration of Vehicle Viewed from Aft Section



Figure 20: Landed Configuration of Payload Section and Main Parachute Viewed from Payload Section

2.4.1.2 Payload

After the documentation of the launch vehicle recovery, the payload was investigated to identify the cause of failure. Deployment of the payload was caused manually to identify the issue of the payload becoming stuck within the bay (Figure 21).



Figure 21: Demonstration of Intended Payload Deployment

Then, the elevator, rudder, and propeller motors were actuated using the remote controller to verify functionality after flight. These systems were functional, demonstrating that the payload would likely have functioned nominally if deployment had succeeded.



Figure 22: Demonstration of Elevator Function After Flight



Figure 23: Demonstration of Rudder Function After Flight



Figure 24: Demonstration of Propellor Function After Flight



2.4.2 Descent Values

GPS data from the Eggfinder Mini GPS, located in the nosecone of the launch vehicle, was recorded prior to launch and following landing of the launch vehicle (Table 3). The drift of the launch vehicle was computed using these coordinates, yielding a drift of 254 ft, which is well below the 2500 ft maximum.

Location	GPS Location
Launch Pad	27.93474° N, 80.70837° W
Landing Site	27.93424° N, 80.70892° W
Total drift = 254 ft	

Table 3: Telemetry Locations at Launch and Landing of the Launch Vehicle with Drift

Using the altitude and velocity profile data from main altimeter, the Stratologger CF, the apogee of the flight was calculated along with the average drogue and main descent rate upon landing. The drogue and main descent rates deviated from the predicted simulation by 3.4% and 0.6% respectively (Table 4). This increase in descent rate led to a decrease in the descent time from the predicted time by 7.9 s, or 10.4%.

Parameter	Stratologger CF	OpenRocket	Error
Apogee Altitude	4671 ft	4625 ft	1.0%
Drogue Descent Rate	95.6 ft/s	92.1 ft/s	3.8%
Main Descent Rate	16.4 ft/s	16.3 ft/s	0.6%
Descent Time	67.9 s	75.8 s	10.4%

Table 4: Descent Value Comparison Between the Main Altimeter and Simulation

With the descent rates and the mass of each launch vehicle section, the kinetic energy at landing for each section was calculated, with maximum kinetic energy occurring for the payload section with a value of 66.55 ft-lbf, which is under the 75 ft-lbf requirement (Table 5).

Section	Mass at landing (lbs)	Drogue Descent rate (mph)	Main descent rate (mph)	Kinetic Energy (ft-lbf)
Payload	15.92	62.7	11.2	66.55
Central	6.13	62.7	11.2	25.61
Aft	11.35	62.7	11.2	47.45

Table 5: Kinetic Energy Results

2.5 Payload Functionality

2.5.1 Functional Systems

2.5.1.1 Mechanical Components

The wing and all control surfaces rolled properly and allowed for the payload to be loaded into the launch vehicle. However, the wing caused the payload to get lodged in the launch vehicle when the payload door opened, so the payload did not deploy. When the wing unfurled, it pressed against the inside of the launch vehicle, preventing the payload from deploying.

After removing the payload from the launch vehicle, all mechanical system worked properly. The propeller, elevator, and rudder systems were tested, and all were functional. The payload also did not sustain any structural damage to the wing, control surfaces, or fuselage.



2.5.1.2 Electrical Systems

2.5.1.2.1 Microprocessor Subsystem

All of the components of the microprocessor subsystem functioned as intended. The sensor suite in conjunction with the Raspberry Pi successfully logged data. Launch was detected and the flight controller subsystem was activated. This was verified through the recovery of the Raspberry Pi's stored data, following payload recovery (2.5.1.3.1 Raspberry Pi).

2.5.1.2.2 Flight Controller Subsystem

Ultimately, the flight controller subsystem performed its function successfully despite the occurrence of some off-nominal events (2.5.2.1.2 Electrical Failures). All of the components of the flight controller subsystem functioned as intended except for the FPV camera and GPS.

The components of this subsystem, the video transmitter, 2.4 GHz receiver, ESC, propeller motor, rudder servo, and elevator servo, all functioned as intended. With respect to the radio controller components of this subsystem, although the payload did not deploy, these systems were verified as functioning through ground testing prior to launch of the vehicle and immediately after the recovery of the launch vehicle (2.4.1.2 Payload). Additionally, the payload retention servos unlocked remotely, demonstrating that radio control was achieved. The functionality of the video transmitter was verified through the reception of video at the ground station. Due to the camera disconnecting from the flight controller, a camera view was not achieved. However, telemetry data was still able to be transmitted and received. The video signal was received up to an altitude of approximately 4625 ft, which is 81% of the predicted maximum range of video transmission.

2.5.1.2.3 Payload Retention Subsystem

Electrically, this subsystem functioned as intended. When the flight controller received the appropriate radio arming signal, the servos retracted at 400 ft. While the payload did not deploy successfully, upon recovery of the launch vehicle, the servos of the payload retention mechanism were found to be retracted, indicating successful function.

2.5.1.2.4 Ground Station

All of the components of the ground station functioned successfully. The video receiver and laptop combination used to receive video from the payload displayed video for the majority of the duration of the mission, only losing signal when the launch vehicle was near apogee. The 2.4 GHz transmitter successfully sent a signal to unlock the payload retention mechanism, demonstrating intended functionality, and would have controlled the flight of the payload had it deployed.

2.5.1.3 Software Systems

2.5.1.3.1 Raspberry Pi

The Raspberry Pi functioned as intended. It was able to collect data from the sensor suite, log flight information, and detect launch. The flight controller was also activated. Figure 25, Figure 26, and Figure 27 show the sensor data recovered from the launch.

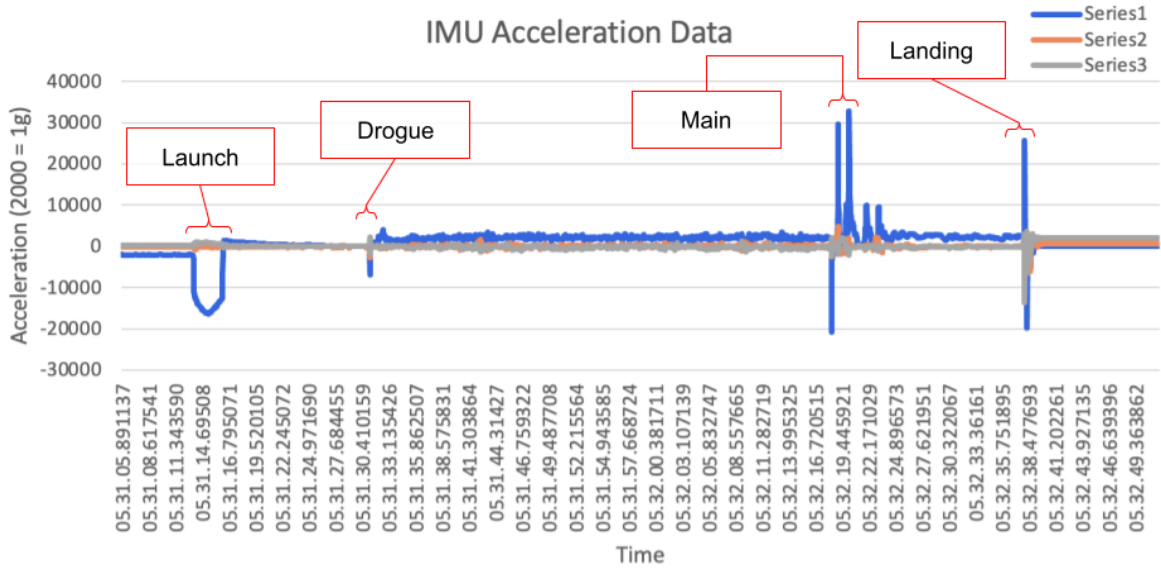


Figure 25: IMU Acceleration Data

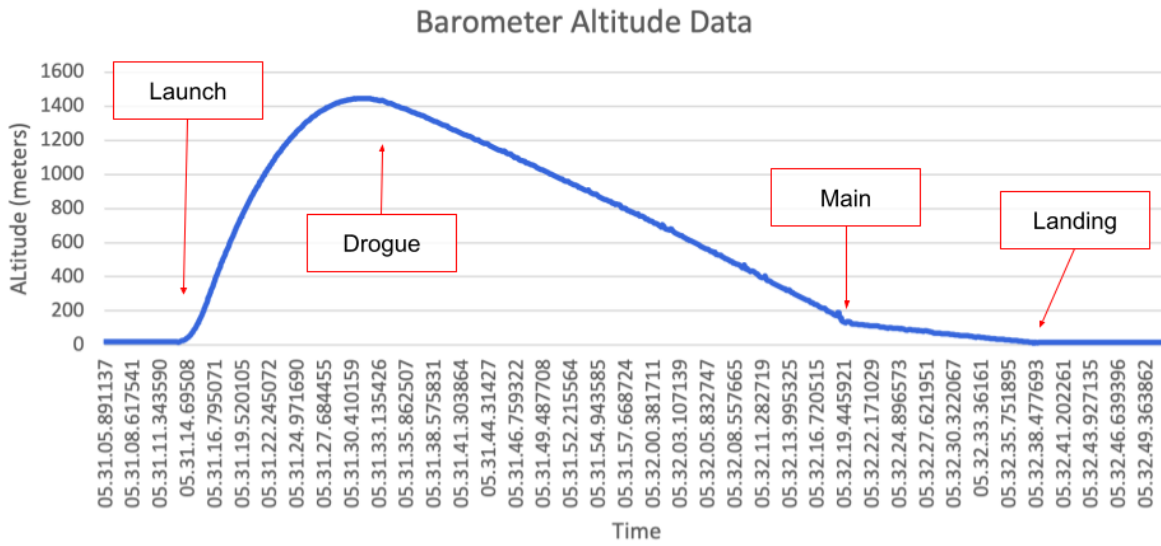


Figure 26: Barometer Altitude Data

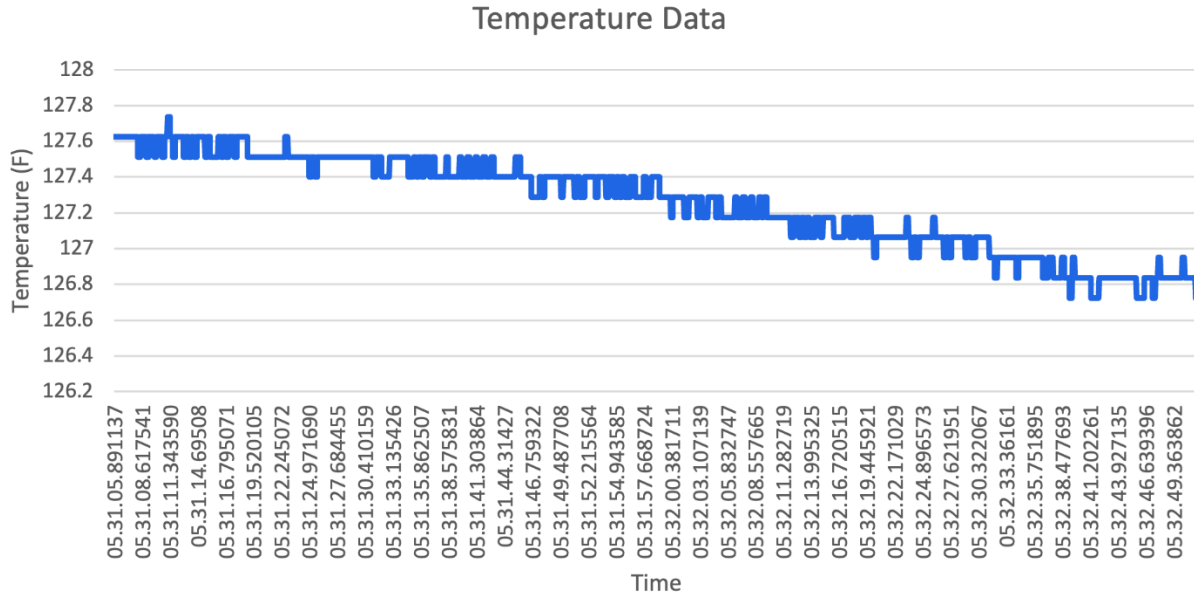


Figure 27: Temperature Data

All three figures show the same time frame of the data log, zoomed in on the launch. Timestamps are formatted as HH.MM.SS.millisecond. The series in Figure 25 represent the x, y, and z axes, respectively. The x axis is parallel to the length of the launch vehicle, and thus was the axis reporting the bulk of the acceleration forces from launch, parachute deployments, and landing. The units reported by the IMU can be converted to g-forces following the conversion 2000 units = 1 g. This conversion was verified through testing (P-A-11).

There was no five second period of g-forces larger than 9gs, meaning that according to the survivability criteria, the STEMnauts survived the flight. 9gs was not exceeded for more than a few milliseconds each time.

The altitude data, adjusted for temperature readings, is consistent with readings from the launch vehicle altimeters, reporting an apogee of 4685 ft.

The temperature on the payload never exceeded 132.2 °F (this maximum was reached at a time prior to the section shown in Figure 27), meaning the payload was within a safe temperature range the entire mission, and nothing was turned off.

2.5.1.3.2 Flight Controller

As discussed in 2.5.1.2.2 Flight Controller Subsystem, the flight controller did function correctly. Despite the FPV camera failing, a live feed was still sent to the ground with telemetry information. The flight controller did respond to ground control, moving the motor, rudder, elevator, and retention system servos, opening the payload bay door at 400 ft.

2.5.1.3.3 Ground Station

The ground station successfully displayed the live video feed while it had contact with the payload. Additionally, Mission Planner was successfully used to set up and calibrate the flight controller's functionality prior to the launch date.



2.5.2 Off-Nominal Events

2.5.2.1 Hardware Failures

The only mechanical system that failed was the wing. The wing caused the payload to become lodged in the launch vehicle and prevented the payload from deploying. Due to the payload not deploying, full payload functionality was unable to be demonstrated.

The deployment mechanism was tested in the first vehicle demonstration flight. The mechanism operated successfully during that flight, so it was determined that the possibility of the payload not deploying was highly unlikely.

2.5.2.1.2 Electrical Failures

The only electrical failures occurred in the flight controller subsystem. As stated previously, the FPV camera and GPS failed to function as intended.

The camera disconnected at its soldered connection points, likely due to the force of launch. However, as the payload was to remain in line of sight, this would not have been an issue for flying the payload had it deployed successfully. Video with telemetry data was still transmitted to the ground station as the video transmitter was functional. As stated previously, the video signal was received up to an altitude of approximately 4625 ft.

The GPS was unable to connect to any satellites. This failure mode was likely caused by satellite signal attenuation due to the carbon fiber of the payload. As such, positional data was unable to be relayed to the ground station. However, positional data is not deployment or flight critical, as such, this failure would have been tolerated had the payload successfully deployed.

2.5.2.2 Software Failures

There were no software failures.

2.6 Payload Hardware Damage

2.6.1 Mechanical Hardware

None of the mechanical systems were damaged. The payload returned to the ground safely inside of the launch vehicle.

2.6.2 Electrical Hardware

The FPV camera was the only electrical component damaged. This damage was due to its unplanned and seemingly forceful disconnection from the flight controller. The extent of this damage included tearing the copper pads from the camera's soldered connection points. Because there is not enough surface area to adhere conductive copper tape to the pads, a replacement camera will be ordered to replace its irreparably damaged counterpart.

2.7 Lessons Learned

Ensure that the GPS is positioned such that minimal signal attenuation can occur due to the carbon fiber, increasing the likelihood of a GPS to satellite connection. Use a connector for the camera instead of soldered connection as a connector will be less likely to fail due to broken solder connection.

Ensure that the interior of the payload bay is as smooth as possible and try to attain a smoother surface on the wing to ensure that the wing does not lodge the payload in the launch vehicle.